Neuron, Vol. 18, 613–622, April, 1997, Copyright ©1997 by Cell Press

aex-3 Encodes a Novel Regulator of Presynaptic Activity in C. elegans

Kouichi Iwasaki,* Jane Staunton,†‡ Owais Saifee,† Michael Nonet,† and James H. Thomas*
*Department of Genetics
University of Washington
Seattle, Washington 98195
†Department of Anatomy and Neurobiology
Washington University School of Medicine
St. Louis, Missouri 63110

Summary

C. elegans *aex-3* mutations cause pleiotropic behavioral defects that are suggestive of reduced synaptic transmission. *aex-3* mutations also show strong genetic interactions with mutations in *unc-31* and *unc-64*, two other genes implicated in synaptic transmission. Physiological and pharmacological studies indicate that *aex-3* defects are presynaptic. In *aex-3* mutants, the synaptic vesicle–associated RAB-3 protein aberrantly accumulates in neuronal cell bodies and is reduced in synapse-rich axons. This localization defect is specific to RAB-3, since other synaptic proteins are localized normally in *aex-3* mutants. *aex-3* encodes a 1409 amino acid protein with strong homology to DENN, a human protein of unknown function. In C. elegans, *aex-3* is expressed in all or nearly all neurons. These results suggest that AEX-3 is a novel regulator of presynaptic activity that interacts with RAB-3 to regulate synaptic vesicle release.

Introduction

Synaptic vesicle release at presynaptic terminals is a highly regulated process that is important for communication between neurons and at the neuromuscular junction. Several steps appear to be important for the process (reviewed by Südhof, 1995). First, synaptic vesicles containing neurotransmitter accumulate at specialized regions of the presynaptic membrane. Once there, docking and priming processes are thought to be required to prepare these vesicles for the rapid exocytosis that is characteristic of excitable cells. Finally, Ca^{2+} influx stimulates the exocytosis event. A variety of proteins have been implicated in this process. Of specific interest for this paper are members of the small GTP-binding family called rab proteins. Various members of the rab family have been shown to regulate vesicular transport steps in neuronal and nonneuronal cells (reviewed by Ferro-Novick and Novick, 1993). A subgroup of the rab family, the rab3-related proteins, appear to be specifically important in secretory events in excitable cells. Rab proteins alternate between a GTP-bound state that is associated with vesicles and a GDP-bound state that is not associated with vesicles (Fischer von Mollard et al., 1991; Fischer von Mollard et al., 1994a; Stahl et al., 1994). These two states are thought to regulate vesicle exocytosis, though the precise role of rab proteins remains unclear.

Many of the proteins that regulate neuronal synaptic vesicle release have been identified by biochemical methods. These methods of identification typically require either direct interaction between these proteins and synaptic vesicles or some prior knowledge of the biochemical function of the proteins. In addition, biochemical analysis has limited potential for testing whether a protein is required for synaptic function in vivo. The utility of a genetic approach to the regulation of secretion is demonstrated by the remarkable success of such analysis in yeast (Ferro-Novick and Novick, 1993). For example, the key role of rab proteins in specific steps of vesicle transport in vivo has been demonstrated by analysis of temperature-sensitive mutations of the rab-encoding genes *sec4* and *ypt1* (Salimen and Novick, 1987; Segev et al., 1988).

C. elegans is well suited to a genetic analysis of neuronal synaptic transmission. C. elegans has a simple nervous system of 302 neurons in the hermaphrodite. Genetic analysis is facilitated because mutants with severely perturbed general neuronal function are often viable. Nevertheless, C. elegans neurons regulate a wide range of behaviors and appear in many ways to function similarly to vertebrate neurons. Specifically, several steps in the mechanism of vertebrate synaptic vesicle function are known to be conserved in nematodes. Synaptic vesicles are transported to presynaptic sites by a kinesin-like protein (Hall and Hedgecock, 1991; Okada et al., 1995). Many vertebrate neurotransmitters are found in *C. elegans*, and these are synthesized and loaded into vesicles by similar proteins (Alfonso et al., 1993, 1994; McIntire et al., 1993; Y. Jin, personal communication). Finally, synaptic vesicle exocytosis is regulated by nematode homologs of synaptotagmin (Nonet et al., 1993), Munc-18 (Gengyo-Ando et al., 1993; Hata et al., 1993), Munc-13 (Maruyama and Brenner, 1991; Brose et al., 1993), p145–CAPS (Livingstone, 1991; Walent et al., 1992), and rab3 (Nonet et al., unpublished data).

We and others previously identified *aex-3* mutants based on specific behavioral defects (Thomas 1990; Avery 1993). Here, we report that *aex-3* mutants have a variety of behavioral, physiological, and pharmacological abnormalities that are consistent with a generalized defect in presynaptic activity. We present evidence that *aex-3* is required for synaptic localization of the product of *rab-3*, a rab3 homolog in C. elegans. Finally, we report that *aex-3* encodes a predicted protein of 1409 amino acids with strong similarity to a human protein of unknown function called DENN. These results suggest that *aex-3* encodes the defining member of a protein family not previously implicated in synaptic vesicle release.

Results

aex-3 Mutants Have Pleiotropic Behavioral Defects

aex-3 mutants were first isolated in a screen for altered defecation behavior (Thomas, 1990). *aex-3* alleles have

‡Present address: Department of Genetics, University of Wisconsin, 445 Henry Mall, Madison, Wisconsin 53706.

also been recovered in screens for feeding defects (Avery, 1993) and aldicarb resistance (Miller et al., 1996; Nonet et al., unpublished data; E. Jorgensen, personal communication). We find that the two most prominent defects in *aex-3* mutants are an abnormal defecation motor program and poor male mating efficiency. The C. elegans defecation motor program consists of a stereotyped series of three muscle contractions (Thomas 1990). First, posterior body-wall muscles contract (pBoc) and then relax, causing gut contents to accumulate near the anus. Three to four seconds later, anterior body-wall muscles contract (aBoc) to pressurize the gut contents. Finally, specialized enteric muscles contract to expel the gut contents from the anus (Exp). In all five *aex-3* mutants analyzed (*ad418*, *sa5*, *ad696*, *n2166*, and *y255*), pBoc appeared normal, but only 10%–20% of defecation motor program cycles had a visible aBoc or Exp (hence the gene name *aex*). In a quantitative mating assay, *aex-3* males sired far fewer cross progeny than wild-type males (see Experimental Procedures). Direct observation showed that *aex-3* mutant males displayed mating behavior less frequently when they encountered hermaphrodites (data not shown). In addition to these severe defects, *aex-3* mutants had other mild behavioral defects. *aex-3(ad696)* and *aex-3(sa5)* mutants retained slightly more eggs than the wild type, indicative of a mild egg-laying defect. Finally, *aex-3* mutants intermittently displayed exaggerated sinusoidal bends of the body during locomotion, a phenotype that was most pronounced in *aex-3(y255)*. No obvious *aex-3* allelic series could be constructed based on the severity of the various behavioral defects. The range of defects observed in *aex-3* mutants suggests a general nervous system abnormality.

aex-3 Has Strong Genetic Interactions with Other Synaptic Mutants

Additional evidence suggesting a synaptic function for *aex-3* comes from genetic interactions affecting dauer formation. The dauer is an alternative larval form that is induced in response to harsh environmental conditions (reviewed by Thomas, 1993). The dauer larva can survive for several months without feeding before resuming development. Dauer formation is controlled by a neuronal circuit, and unregulated dauer formation can result from defective nervous system function.

In the course of genetic analysis of *aex-3*, we found that double mutants between *aex-3* and either *unc-31* or *unc-64* displayed strong dauer formation–constitutive (Daf-c) phenotypes. *unc-31* encodes a nematode homolog of p145, a calcium-dependent activator of secretion (Livingstone 1991; Walent et al., 1992), and *unc-64* encodes a homolog of syntaxin (M. Nonet, unpublished data). Both of these proteins are implicated in synaptic vesicle release. Whereas none of the single mutants had an obvious Daf-c phenotype, double mutants in all possible combinations among *aex-3*, *unc-31*, and *unc-64* alleles displayed a strong Daf-c phenotype (Figure 1). These results suggest that *aex-3*, *unc-31*, and *unc-64* function together in related processes.

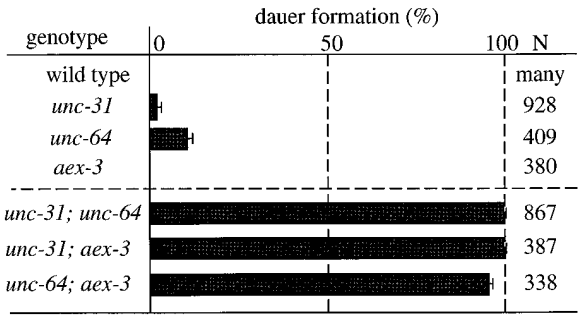

Figure 1. Synthetic Dauer Formation Caused by *unc-31*, *unc-64*, and *aex-3* Mutations

Constitutive dauer formation in single and double mutants of *unc-31(u280)*, *unc-64(e246)*, and *aex-3(y255)* alleles. For each genotype, three assays were performed at 25°C, and the mean is shown. N is the total number of animals assayed for each genotype, and the bars show the SEM. All possible combinations among *unc-64(e246)*, *unc-64(md130)*, *unc-31(e169)*, *unc-31(e928)*, *unc-31(u280)*, *aex-3(ad418)*, *aex-3(sa5)*, *aex-3(ad696)*, *aex-3(n2166)*, and *aex-3(y255)* were tested, and results were consistent in every case.

Electropharyngeogram Indicates Synaptic Transmission Defects in *aex-3* Mutants

To test more directly for synaptic transmission defects in *aex-3* mutants, we examined activity in the pharyngeal nervous system of these animals using an extracellular recording technique developed by Raizen and Avery (1994). This technique allows for visualization of currents intrinsic to muscle action potentials as well as those resulting from synaptic input (Figure 2). Currents elicited by two distinct motor neurons can be identified. First, we examined inhibitory muscle transients produced by the motor neuron M3, which promotes the repolarization of pharyngeal muscles (Avery et al., 1995). Wild-type animals exhibited between three and five distinct M3-induced transients during each pharyngeal pump. In contrast, in *aex-3* mutants, M3-induced transients were more variable and were often difficult to identify because they were smaller in amplitude (Figure 2). The length of the pharyngeal pump was also longer in *aex-3* mutants (Figure 2 legend; $P < 0.01$). As M3 is thought to regulate the duration of the pharyngeal muscle contraction, the increase in pump length is indicative of a reduction in the M3 function.

We also examined MC-induced transients in the wild-type and in *aex-3* mutants. The MC motor neuron is thought to trigger the contraction of pharyngeal muscles (Raizen et al., 1995), and its activation can be seen as a single transient preceding many pumps (Figure 2). However, in *aex-3* animals, MC-induced transients often occurred in bursts preceding pharyngeal pumps. These MC-induced transients were variable in amplitude and number. Bursts of probable MC activity that did not correlate to a pharyngeal pump were also observed in *aex-3* records (Figure 2). These probably represent failed attempts by MC to trigger a muscle action potential. Thus, MC and M3 functions are abnormal in *aex-3* animals. In particular, the characteristics of the M3 and MC transients suggest that transmitter release is less synchronous and less efficacious in *aex-3* animals than in the wild type.

Pharmacological Analysis of *aex-3* Mutants Suggests a Defect in Presynaptic Function

To test further whether *aex-3* mutants have defects in synaptic transmission, we measured sensitivity to the

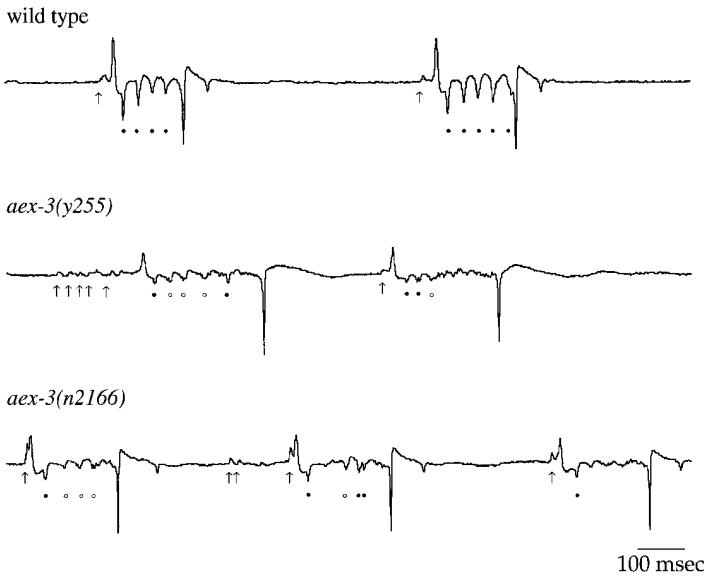

Figure 2. Synaptic Transmission in the Pharynx Is Abnormal in *aex-3* Mutants

Characteristic electropharyngeogram recordings from wild-type and *aex*-3 animals. Voltage is displayed with respect to time (milliseconds). Transients resulting from both muscle action potentials and from synaptic transmission from two motor neurons to pharyngeal muscle are visible in the records (Raizen and Avery, 1994; Raizen et al., 1995). M3 motor neuron–induced transients identified by a peak detection algorithm (closed circles) and those undetected by the algorithm (open circles) are labeled. MC-induced transients are also labeled (arrows). Bursts of MC activity preceding a pharyngeal pump are visible in both *aex-3* records. Other notable differences between the wild type and *aex-3(y255)* mutant are as follows: pump duration (ms), 152 ± 3 [wt], 213 ± 5 [*aex-3*]; number of M3-induced transients per pump, 4.0 ± 0.1 [wt], 2.3 ± 0.2 [*aex-3*]; mean amplitude of M3-induced transients normalized to amplitude of the R-phase transient, 31% ± 1% [wt], 18% ± 1% [*aex-3*]; pumps with MC bursts, 7% [wt], 43% [*aex-3*]; and frequency of failure of MC to induce pump, 0.14 [wt], 0.5 [*aex-3*]. Analysis is based on recordings containing at least 10 pumps from at least 11 animals. Means are represented by ±SEM. See Experimental Procedures for other definitions.

acetylcholinesterase inhibitor aldicarb. Resistance to aldicarb results from reduced presynaptic acetylcholine release and is well correlated with defects in synaptic transmission (Nonet et al., 1993; Miller et al., 1996). We found that all *aex-3* mutants resisted paralysis induced by treatment with 0.5 mM of aldicarb for 6 hr (Figure 3A). As a positive control, we tested a mutant of *lev-1*, which encodes a subunit of a nicotinic acetylcholine receptor (Fleming et al., 1993). As expected, the *lev-1* mutant strongly resisted aldicarb in our assay (Figure 3A). The aldicarb resistance of *aex-3* mutants could thus be due to either pre- or postsynaptic defects.

To determine whether the *aex-3* defect is pre- or postsynaptic, we measured sensitivity of *aex-3* mutants to levamisole, an acetylcholine receptor agonist in nematodes (Lewis et al., 1980). We found no significant difference in sensitivity to levamisole (20, 60, and 100 μM) between an *aex-3(n2166)* mutant and the wild type (Figure 3B; data not shown). We also tested other *aex-3* alleles and found similar levamisole sensitivity (data not shown). As expected, the *lev-1* mutant strongly resisted levamisole (Figure 3B), consistent with its postsynaptic defect. These pharmacological assays indicate that *aex-3* mutants are impaired in presynaptic acetylcholine release. Together with the pleiotropic behavioral defects, these results suggest that *aex-3* mutants confer a general defect in presynaptic activity.

RAB-3 Protein Mislocalizes in *aex-3* Mutants

In an attempt to determine how *aex-3* mutations impair presynaptic activity, we examined *aex-3* mutants using antibodies specific for two synaptic vesicle components, SNT-1 (synaptotagmin; Nonet et al., 1993) and RAB-3 (a rab3 homolog, Nonet et al., unpublished data). In the wild-type and in the *aex-3(y255)* mutant, anti-SNT-1 antiserum stained only the synapse-rich axons and not cell bodies (Figure 4), suggesting that SNT-1 is correctly localized to synaptic terminals in the *aex-3* mutant. Anti-RAB-3 antiserum stained predominantly axons in wild-type animals, though faint staining of occasional cell bodies was visible (Figure 4). In contrast, in the *aex-3* mutant, anti-RAB-3 antiserum stained predominantly cell bodies (Figure 4). This observation suggests that *aex-3* is required for proper localization of RAB-3 protein in axons and confirms a general presynaptic defect.

Molecular Analysis of *aex-3*

We used a positional cloning approach to determine the molecular identity of *aex-3*. Genetic map data (see Experimental Procedures) indicated that *aex-3* lies approximately midway between *egl-17* and *unc-1* near the left tip of the X chromosome (Figure 5A). Based on a correlation of the physical and genetic maps from this region, we tested several cosmids for transgenic rescue of the Aex phenotype (Mello et al., 1991). Cosmid C02H7 rescued the Aex phenotype, but two overlapping cosmids, M02A10 and R04F4, did not rescue (Figure 5A). To further narrow the potential *aex-3* region, three λ phage subclones and two plasmid subclones derived from cosmid C02H7 were tested for transgenic rescue (Figure 5A).

A Northern blot probed with the insert from the smallest rescuing clone (pTJ500) revealed a single candidate *aex-3* mRNA of about 5 kb (Figure 5B). Using the same probe, one cDNA clone was isolated from ~300,000 plaques from a cDNA library (Barstead et al., 1991). This cDNA had a 1.7 kb insert and a poly-(A) stretch at one end, suggesting that the insert corresponds to the 3′ end of the *aex-3* mRNA. During this study, the C. elegans Genome Sequencing Consortium completed this region of the X chromosome (Wilson et al., 1994; C. elegans Genome Sequencing Consortium, personal communication). Genefinder analysis of the *aex-3* rescuing region predicted a single gene product (P. Green, personal

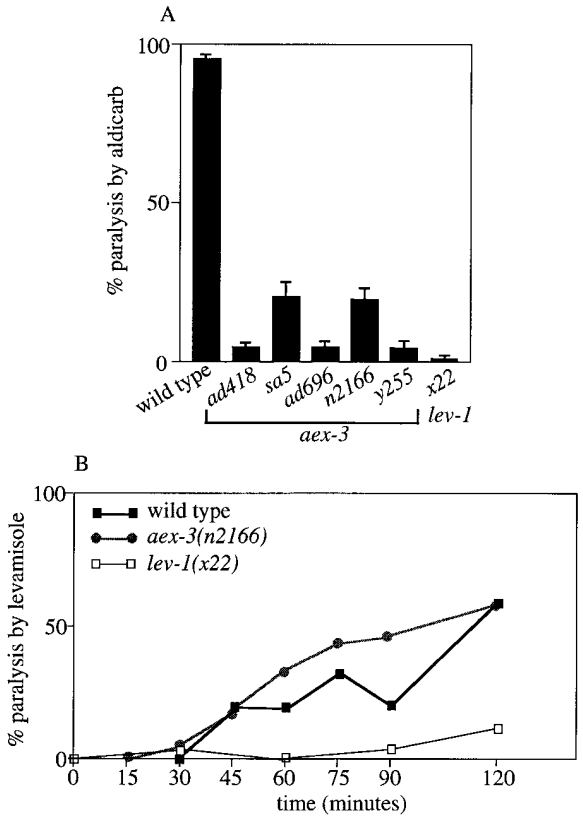

Figure 3. Pharmacological Assays

(A) Aldicarb sensitivities of *aex-3* mutants and the wild type. Aldicarb sensitivities of *aex-3(n2166)* and wild-type animals were first determined at several different doses and times of exposure (data not shown). Based on these assays, a 6 hr exposure to 0.5 mM aldicarb was selected because this test readily distinguished wild-type from mutant sensitivity. The genotype of each strain is shown under each bar. Twenty animals per plate were tested (3 plates for *lev-1* and 10 plates for the others). At the top of each bar, the SEM is shown. (B) Levamisole sensitivities of an *aex-3* mutant and the wild type. The x-axis shows time (minutes) after exposing animals to 60 μM levamisole. The y-axis shows the percentage of paralyzed animals. Twenty animals per plate were tested (three plates per strain).

communication). With the Genefinder prediction as a guide for primer selection, we used reverse transcription coupled to the polymerase chain reaction (RT–PCR) to determine the sequence of the remainder of the *aex-3* mRNA. This analysis showed that the entire *aex-3* mRNA is 4.6 kb in size and is trans-spliced to an SL1 leader sequence at its 5′ end (Figure 5C). This mRNA has a single long open reading frame of 1409 amino acids (Figure 6). *aex-3* consists of 19 exons (Figure 5C), and its putative 5′ and 3′ untranslated regions are 53 and 332 nucleotides, respectively (data not shown). To confirm that this transcript corresponds to *aex-3*, we generated frameshift mutations predicted to affect the open reading frame. One of the frameshifts affects codon 418, and the other affects codon 687 (see Figure 6). We found that these two mutant genes failed to rescue the Aex phenotype in transgenic *aex-3* animals (Figure 5C).

A BLASTP search using the AEX-3 protein sequence identified a single protein with substantial homology to AEX-3. This human protein is called DENN (Genbank accession U48254) and has no known function. Three regions of high similarity between DENN and AEX-3 are separated by two large, less-conserved domains, and the AEX-3 C-terminus includes an extension of 295 amino acids not found in DENN (Figure 6). Some short hydrophobic stretches were predicted for AEX-3 (Kyte and Doolittle, 1982), but none were convincing transmembrane domains. One portion of AEX-3 is proline rich (amino acids 925–1069) and has the potential to function in SH3 binding or cytoskeleton association (Yu et al., 1994), but this region is not well conserved in DENN. Consistent with our identification of the *aex-3* gene, we found a mutation in *aex-3(ad696)* that changes lysine 989 to arginine (Figure 6). We conclude that *aex-3* encodes a conserved protein not previously implicated in synaptic function.

To examine the expression pattern of *aex-3*, we constructed an *aex-3::gfp* fusion gene. In this construct, a 1.3 kb fragment of the *aex-3* promoter was fused in frame with the *gfp* coding sequence (Figure 5C). To facilitate identification of cells, a protein nuclear localization signal was included in the construct (A. Fire, S. Xu, J. Ahm, and G. Seydoux, personal communication). GFP fluorescence was detected in all or nearly all neurons. Figure 7 shows the fluorescence detected in the major ganglia near the nerve ring, neurons in the ventral cord, and neurons in the tail ganglia. In Figure 7B, the general haze of fluorescence arises from the many neurons located out of the focal plane of the photograph. One segment of the ventral nerve cord is seen in Figure 7B. Over its length, the ventral cord contains 47 neurons (not including the retrovesicular ganglia; White et al., 1976), and we detected GFP fluorescence in 45.7 ± 1.9 cells (N = 9), suggesting that all ventral cord neurons express AEX-3. The expression pattern of the *aex-3::gfp* construct is consistent with the immunostaining pattern with anti-RAB-3 antibody, since mislocalization of RAB-3 was found generally in neurons of the *aex-3* mutants. In some animals, intestinal cells fluoresced variably (Figure 7).

Discussion

aex-3 Mutants Have a Presynaptic Defect

Various experimental observations indicate that AEX-3 functions presynaptically to regulate transmitter release in many classes of neurons. *aex-3* mutants are abnormal in a wide variety of behaviors, suggesting that the defects are not limited to a single neurotransmitter system. Additionally, defects in excitatory MC (probably cholinergic; Raizen et al., 1995) and inhibitory glutamatergic M3 synaptic transmission are observed in extracellular recordings of pharyngeal activity. While neither the behavioral defects nor the pharyngeal recordings address whether the defect in transmission in *aex-3* mutants is pre- or postsynaptic, several other lines of evidence support a presynaptic function for AEX-3. First, the combined sensitivities of *aex-3* mutants to a cholinergic receptor agonist and to an acetylcholinesterase inhibitor support a presynaptic defect. Second, the fact that expression of *aex-3* is limited to neurons suggests a presynaptic site of action at neuromuscular junctions. Third,

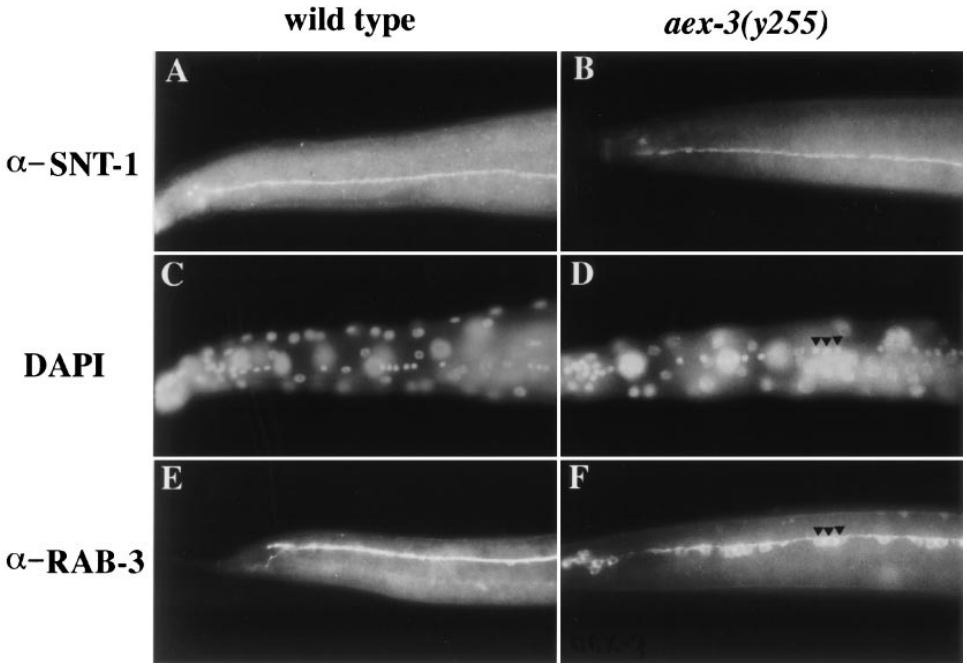

Figure 4. Localization of SNT-1 and RAB-3 in *aex-3* Mutants

Wild-type (A) and *aex-3(y255)* (B) animals stained with anti-synaptotagmin antisera. In both wild-type and *aex-3* mutants, synaptotagmin immunoreactivity was restricted primarily to the ventral cord where many neuromuscular synapses are found. DAPI staining of the wild type ([C], the same animal as [A]) and *aex-3* mutant ([D], the same animal as [F]) shows cell bodies. Wild type (E) and *aex-3(y255)* (F) animals stained with anti-RAB-3 antiserum. Specificity of the antiserum was demonstrated by absence of staining in *rab-3* mutants. In wild-type animals, immunoreactivity is restricted primarily to the ventral cord. In contrast, in *aex-3* animals, much of the RAB-3 immunoreactivity is located in neuronal cell bodies. In (D) and (F), closed arrows indicate examples of cells showing this pattern. Similar staining was observed for *sa5* and *n2166* (data not shown).

the mislocalization of the synaptic vesicle–associated protein RAB-3 in *aex-3* mutants indicates a presynaptic function for AEX-3. Thus, behavioral, physiological, pharmacological, molecular, and cellular evidence suggests that AEX-3 is a panneuronal regulator of synaptic transmission.

Genetic Interactions among *aex-3*, *unc-31*, and *unc-64*

All double-mutant combinations of *aex-3*, *unc-31*, and *unc-64* displayed a synthetic Daf-c phenotype, suggesting that these genes function in regulating dauer formation. Identified sensory neurons are known to regulate dauer formation (Bargmann and Horvitz, 1991; Schackwitz et al., 1996), but little is known about synaptic events in this process. Our results suggest that certain defects in synaptic transmission can result in a Daf-c phenotype. We hypothesize that *aex-3*, *unc-31*, and *unc-64* each function in different aspects of synaptic vesicle exocytosis. Mutations in each gene may impair synaptic function to a degree that is insufficient to induce dauer formation. However, combinations of these mutations may reduce synaptic function below some threshold, resulting in a strong Daf-c phenotype.

AEX-3 May Regulate RAB-3 Function

The specific failure of RAB-3 protein to localize to synaptic regions in *aex-3* mutants suggests that *aex-3* in some way regulates *rab-3* function. Consistent with this, the electrophysiological defects of *rab-3* and *aex-3* mutants are very similar (Nonet et al., unpublished data). However, behavioral defects point to roles for *aex-3* beyond regulating *rab-3* activity. *aex-3* mutants have abnormal defecation motor steps and slight egg-laying defects that are not observed in the *rab-3* null mutant (Nonet et al., unpublished data). In addition, male mating is more severely affected in *aex-3* mutants. One possible explanation for these behavioral differences is that mislocalization of RAB-3 in *aex-3* mutants causes abnormalities beyond those resulting from the loss of RAB-3 function. A more likely possibility is that *aex-3* functions to regulate other proteins in addition to RAB-3. One intriguing possibility is that *aex-3* is required for the proper localization of other rab proteins associated with synaptic vesicles such as rab5 (deHoop et al., 1994; Fischer von Mollard et al., 1994b).

Mislocalization of RAB-3

Furthering our understanding of AEX-3 will require determining how *aex-3* mutations cause mislocalization of RAB-3 protein. We consider three likely possibilities. One possibility is that geranylgeranyl transferase (GGT) activity is impaired in *aex-3* mutants. Rab3 is known to be geranylgeranylated at the C-terminus, and this modification is important for rab3 attachment to synaptic vesicles (Johnston et al., 1991). GGT consists of two subunits, components A and B (Seabra et al., 1992; Andres et al., 1993). Component B has GGT activity,

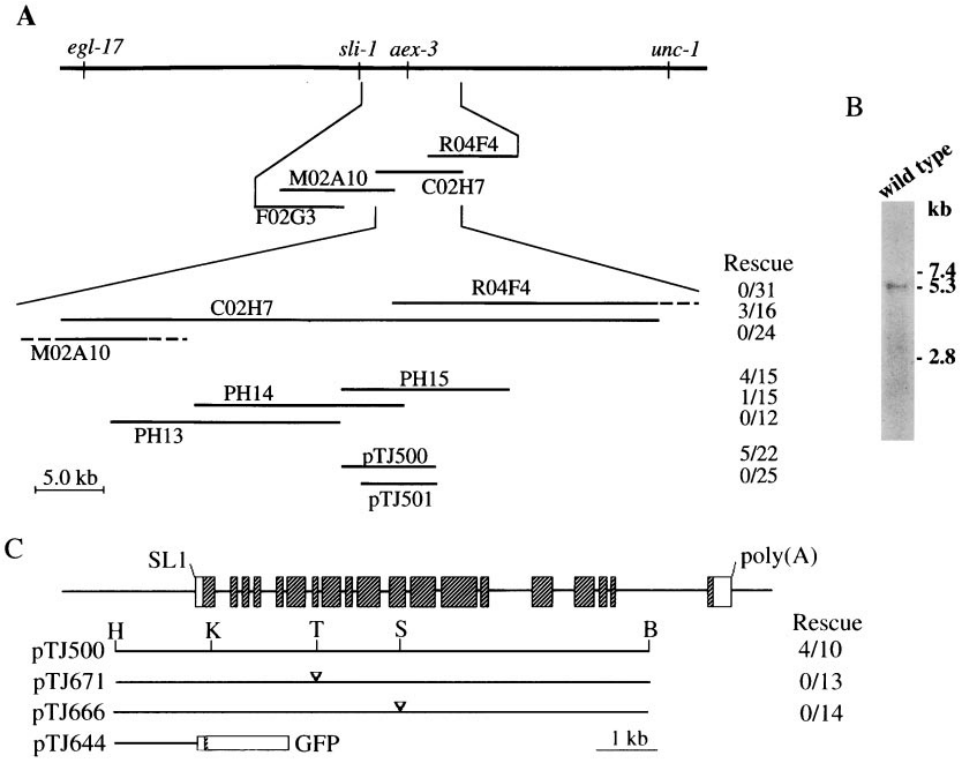

Figure 5. Genetic and Physical Map Near *aex-3*

(A) The top section shows the genetic map near the left end of the X chromosome. Below, four cosmids that span the *aex-3* region are shown (F02G3, M02A10, C02H7, and R04F4). The lower part is a magnified view of the physical map. The extents of three cosmid inserts, three λ phage inserts, and two plasmid inserts are shown. To the right of each clone name, the frequency of *aex-3(ad418)* rescue is shown for each clone (number of rescued animals per number of F1 Rol transformants). The marker used was *rol-6*. *aex-3* is transcribed from right to left.

(B) Northern blot of *aex-3* mRNA. Poly-(A) RNA from wild-type animals was separated by agarose gel electrophoresis, blotted to a Nitran membrane, and hybridized with an *aex-3* DNA probe (pTJ500). Sizes of markers are shown on the right.

(C) The *aex-3* gene structure (top bar). Exons are indicated by boxes. The shaded and open boxes are the translated and untranslated regions, respectively. The trans-splicing and poly(A) sites are also indicated. The plasmids used for transgenic assays are shown below, along with their rescue frequencies. These experiments are additional to those in (A). In these experiments, *lin-15* was used as a marker instead of *rol-6*. Restriction enzyme sites are H, HindIII; K, KpnI; T, Tth111I; S, SpeI; and B, BglII. Inverted triangles indicate the sites of introduced frameshifts. The open box is the GFP coding region.

and component A is thought to present rab3 protein to component B (Andres et al., 1993). AEX-3 has no homology to component A or B and therefore is unlikely to encode these functions in C. elegans. It remains possible that *aex-3* is less directly required for this process.

A second possibility is that RAB-3 guanine–nucleotide exchange activity is impaired in the *aex-3* mutant. Exchange of GDP for GTP on rab3 is thought to activate attachment to synaptic vesicles (Stahl et al., 1994). Guanine–nucleotide exchange on rab3 is promoted by MSS4 in mammals (Burton et al., 1994). AEX-3 has no homology to MSS4 or other guanine–nucleotide exchange factors, but it might form a novel class of nucleotide exchange factor, or it might be required indirectly for this process.

A third possibility is that AEX-3 is a RAB-3 binding protein of novel but unknown function. A variety of rab3 binding proteins have been identified and sequenced. These include rabphilin3a (Shirataki et al., 1993), rabin3 (Brondyk et al., 1995), and GDI (Sasaki et al., 1990). AEX-3 has no homology to any of these rab3 binding proteins, but it might encode a new RAB-3 binding protein that promotes transport of RAB-3 to presynaptic terminals or binding of RAB-3 to synaptic vesicles.

Our work has identified a novel synaptic regulator that impairs synaptic transmission, probably in part by affecting RAB-3 function. Two roles for rab3 protein have been previously suggested: 1) rab3 acts as a negative regulator of vesicle release (Oberhauser et al., 1992; Johannes et al., 1994; Olszewski et al., 1994), or 2) rab3 acts to enhance vesicle release during repetitive stimulation (Geppert et al., 1994a). In C. elegans *rab-3* and *aex-3* mutants, the strength and synchrony of M3 synaptic transmission to pharyngeal muscle is clearly reduced, not increased. Furthermore, *aex-3* mutations act synergistically with other mutations that decrease synaptic transmission. Thus, our experiments are more consistent with roles for RAB-3 and AEX-3 in promoting rather than inhibiting synaptic vesicle release.

Experimental Procedures

Genetic Mapping

Methods for C. elegans culture, genetic analysis (Brenner 1974; Sulston and Hodgkin 1988), and nomenclature (Horvitz et al., 1979) were as previously described. The following mutations were used:

LGIII *unc-64(e246, md130)*

LGIV *unc-31(e169, e928, u280)*

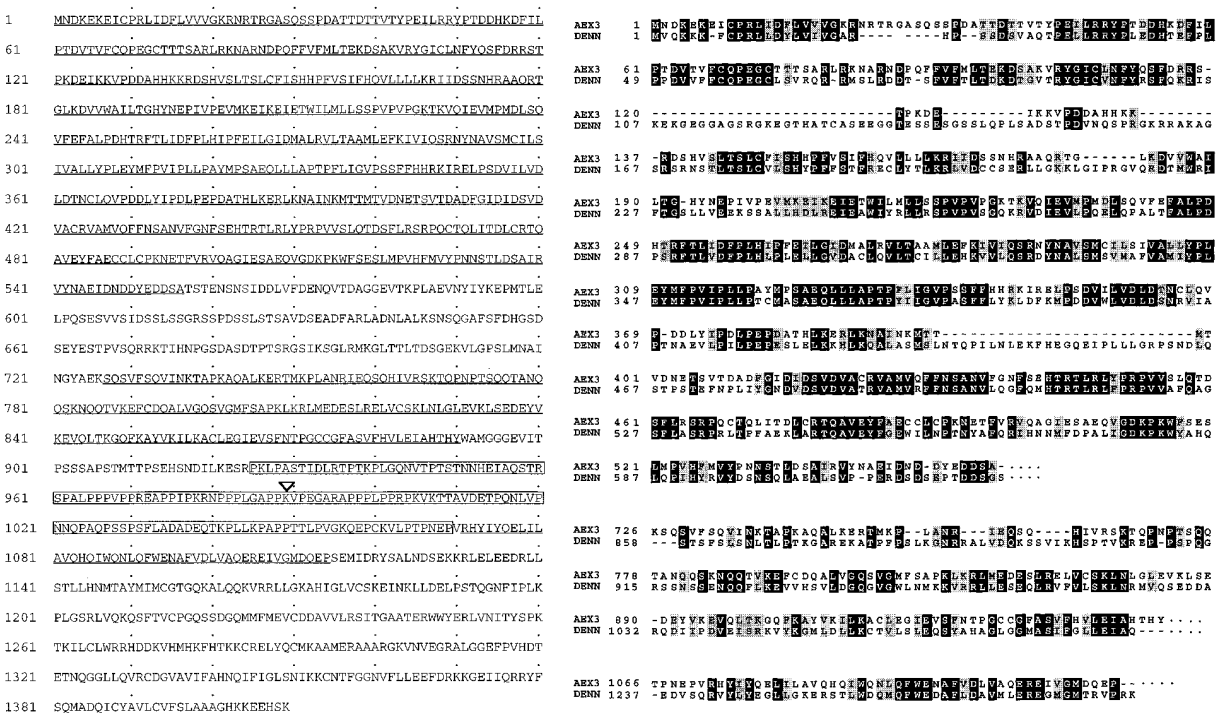

Figure 6. Sequence of the Predicted AEX-3 Protein Amino Acid Number (Left)

The entire protein is 1409 amino acids long. The underlined sequences are the domains with strong homology to DENN. A BLASTP search of the "nonredundant" database in September 1996 revealed a single highly significant hit ($P = 2.0$; e-178). The identity between AEX-3 and DENN is 50.7% in the first domain, 31.7% in the second domain, and 43.2% in the third domain, using the BESTFIT program. One part of the first domain also has weak similarity to a HeLa tumor suppressor gene (HTS-1) (Lichy et al., 1992). The boxed sequence is a proline-rich domain. Lys 989, which is mutated to Arg in *ad696*, is indicated by a triangle. On the right is an alignment of AEX-3 and DENN generated by Clustal W; black boxes indicate amino acid identities, and gray boxes indicate conservative changes.

LGV *dpy-11(e224)*

LGX *egl-17(e1313)*, *aex-3(ad418*, *sa5*, *ad696*, *n2166*, *y255)*, *unc-1(e580)*, *lin-15(n765ts)*.

Genetic mapping of *aex-3* was performed as follows. From *egl-17(e1313) unc-1(e580)/aex-3(sa5)* hermaphrodites, Egl non-Unc recombinant progeny were picked and scored for segregation of the Aex phenotype. Four of nine recombinants were *egl-17 unc-1/egl-17* and the other five recombinants were *egl-17 unc-1/egl-17 aex-3*.

Construction of Double Mutants

For *unc-31; aex-3* double mutants, *unc-31*/+ males were mated with *aex-3* hermaphrodites. From doubly heterozygous F1 hermaphrodites, F2 Aex progeny were picked singly, and from these, F3 Unc progeny were picked. *unc-64; aex-3* mutants were constructed similarly. For *unc-31; unc-64* double mutants, a similar cross was used to generate *unc-31*/+; *unc-64*/+ animals, from which Unc-64 progeny were picked. From confirmed *unc-64* homozygotes, Unc-31 segregants could be distinguished based on their more severe Unc and Egl phenotypes. The resulting *unc-31; unc-64* strains were crossed with N2 males to confirm segregation of the two different Unc phenotypes.

Behavioral Assays

Defecation assays were performed as described (Liu and Thomas, 1994). Male mating assays were performed as described (Hodgkin, 1983). Briefly, six males of the appropriate genotype were mated with six *dpy-11(e224)* hermaphrodites for 24 hr before removing the parents. Cross progeny were counted 3 days later. Six different trials were made for each strain. Male mating efficiencies are as follows, with a reference to the wild type 100%: *aex-3(ad696)*, 33.5%; *n2166*, 14.4%; *y255*, 10.0%; *ad418*, 1.0%; and *sa5*, 0%.

Dauer formation assay conditions were as described (Vowels and Thomas 1992). Twenty adult animals grown at 15° were allowed to lay eggs for 3–5 hr at room temperature. After removing the adults, the plates were placed at 25°C. ~2 days later, dauers and nondauers were counted. Tests showed that recovery from the dauer stage in these strains is very poor at 25°C. Because double mutants containing *unc-64(md130)* grew asynchronously, these strains were observed several times over 24 hr, and dauers and L3 larvae were counted and removed at each time.

Pharmacological Assays

Just before pouring 35 mm plates, aldicarb (100 mM in 70% ethanol) or levamisole (100 mM in water) was added to NG agar at the appropriate concentration. After seeding with bacteria, 20 young adult worms were placed on each of three plates for each time point and drug concentration. Acute effects of the drugs were assessed in a paralysis assay, rather than a chronic growth assay (Nonet et al., 1993; Nguyen et al., 1995). For scoring, animals were classified into three groups based on their movement in response to tapping the plate: complete paralysis, no movement at all; partial paralysis, some movement but no obvious forward or backward locomotion; or no paralysis, forward or backward locomotion. In Figure 3, only animals that were completely paralyzed were plotted. Similar conclusions result from analysis that includes partially paralyzed animals. *lev-1(x22)* animals were chosen as a control because, unlike other strong levamisole-resistant mutants, they are not uncoordinated and are thus comparable to *aex-3* mutants for locomotion.

Microinjection Rescue

Microinjection was carried out as described (Mello et al., 1991). Cosmid or plasmid DNAs were purified using Qiagen columns following the manufacturer's protocol. pRF4 (*rol-6* marker plasmid)

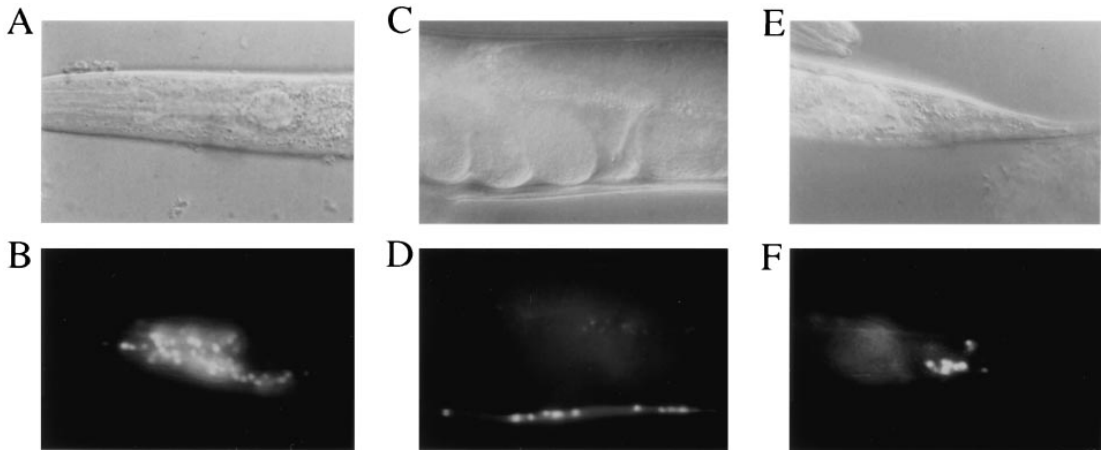

Figure 7. Expression of an *aex-3::gfp* Fusion Construct

The top panels are Nomarski images of animals carrying pTJ644 (an *aex-3::gfp* construct; see Figure 5C). The bottom panels are epifluorescence images of the corresponding regions of the same animals.
(A and B) The head ganglia that surround the nerve ring.
(C and D) A middle segment of body with the ventral nerve cord on the ventral aspect.
(E and F) A posterior tail ganglion. The animal in (C) and (D) is older than those of other panels.

and test DNA were coinjected into *aex-3(ad418)* animals at concentrations of 200 ng/μl and 5–20 ng/μl, respectively. Alternatively, pbHL98 (lin-15 marker) and test DNA were coinjected into *aex-3(ad418) lin-15(n765ts)* animals (Huang et al., 1994). F1 Rol or non-Lin progeny of injected animals were scored for the Aex phenotype by direct observation using a dissecting microscope.

To make strains carrying the *aex-3::gfp* construct, *aex-3(ad418) lin-15(n765ts)* animals were injected with pTJ500 (*aex-3* plasmid, see Figure 5), pTJ644 (*aex-3::gfp* construct), and pbHL98 (*lin-15* marker) at 5 ng/μl, 200 ng/μl, and 20 ng/μl, respectively. To find non-Lin progeny from injected animals, the progeny were grown at 25°C.

Immunocytochemistry

Immunocytochemistry was performed as described (Nonet et al., 1993), except that worms were fixed in a modified Bowin's fixative (0.75 ml saturated picric acid, 0.25 ml formalin, 0.05 ml glacial acetic acid, 0.25 ml methanol, and 0.01 ml B-mercaptoethanol). Antisera against SNT-1 and RAB-3 are described elsewhere (Nonet et al., 1993, and unpublished data).

Electrophysiology

Electropharyngeograms were recorded using an AC preamplifier (designed by David Brumley, University of Oregon) and LabView Acquisition software as previously described (Avery et al., 1995). The bath solution consisted of M9 with occasional addition of 2.5 mM serotonin to stimulate pumping. Young adult hermaphrodites were used for all analysis. Only records with at least 10 pharyngeal pumps were used in analysis. The duration of the pharyngeal pumps was defined as the time from the peak of the E-phase transient to the peak of the R-phase transient (Raizen and Avery, 1994). M3 transients were identified using a peak detection algorithm, which detected negative peaks with an amplitude of >10% of the mean amplitude of the R-phase transients in a record. This algorithm identified >99% of M3 transients visible in wild-type records. MC activity was scored as spikes distinguishable by eye from background occurring within 200 ms preceding a pump. We defined bursts as multiple transients occurring in this interval. MC failures were identified as transients occurring in the absence of a pump.

Nucleic Acid Analysis

Molecular biological methods were essentially as described (Sambrook et al., 1989). PH14 was isolated from a C. elegans genomic λ phage library (Stratagene) probing with both 2.0 and 2.2 kb EcoRI fragments of C02H7, which are not contained in M02A10 or R04F4. PH13 and PH15 were subclones of BglII fragments from C02H7 using the λ DASH II vector (Stratagene). For construction of pTJ500, an 8 kb HindIII to NotI (vector site) fragment from PH15 was cloned into pBluescript SK+ (Stratagene). For construction of pTJ501, a 5.2 kb HindIII to SphI fragment from pTJ500 was cloned into pBluescript SK+. The SphI site was converted to a BamHI site by T4 DNA polymerase treatment and BamHI linker ligation.

aex-3 plasmids carrying frameshift mutations were constructed as follows. pTJ500 was digested with Tth111I, treated with T4 DNA polymerase, and self-ligated, resulting in a 1 base insertion at codon 418 of AEX-3 (pTJ671). Similarly, pTJ500 was digested with SpeI, treated with T4 DNA polymerase, and self-ligated, resulting in a 4 base deletion at codon 687 of AEX-3 (pTJ666). DNA sequencing confirmed the frameshifts in both plasmids.

Total RNA from mixed-stage worms was a gift from D. Birnby. Poly-(A) RNA was isolated by oligo-d(T) cellulose selection. RNA was fractionated by agarose gel electrophoresis and transferred to a Nitran membrane (Schleicher and Schuell) by capillary transfer. Hybridization and washing followed a manual supplied by Schleicher and Schuell. The C. elegans cDNA library was a gift from R. Barstead (Barstead et al., 1991).

A cDNA clone was isolated by in situ hybridization using the pTJ500 insert as a probe. A Bluescript plasmid containing the cDNA insert was generated by the M13 phage excision system (Stratagene). RT–PCR was performed using a 5′ RACE system (Life Technology). Total C. elegans RNA (1 μg) was used to generate first strand cDNA with *aex-3*-specific primers OLG296, OLG297, and OLG298. For internal segments of the cDNA, first strand cDNA was amplified by PCR using *aex-3*-specific primers as described below. For the 5′ end of *aex-3*, the anchor primer provided with the 5′ RACE system was used. In each case, Southern blot hybridization probing with the pTJ500 insert confirmed that the RT–PCR products were specific to *aex-3*. RT–PCR products were cloned into a Bluescript SK+ plasmid. Primer pairs used were as follows: anchor primer–OLG289, OLG290–OLG291, OLG292–OLG293, and OLG294–OLG295. The anchor primer and OLG289–295 (except for OLG294) introduced restriction sites (either SalI, EcoRI, or BamHI), which were used to clone the RT–PCR products. Cloning of PCR products with primers OLG292–OLG293 and OLG294–OLG295 was performed using endogenous EcoRI or BamHI sites on the primers. Primer sequences were:

OLG289—GGAATTCGTCTTTTTGTGGTGAGCATC
OLG290—CGGGATCCAGACGCTCAACTCCTAAAG
OLG291—GGAATTCGGGTTCTGGTATGTTCACTG
OLG292—CGGGATCCGTTTTTGAGTTTGCCCTTCC

OLG293—GGAATTCAGACTTTCATCCTCCATCAG
OLG294—GATGCTTCCGATACACCTAC
OLG295—CGGGATCCTTTGGTCTCGGTGGTAATGG
OLG296—TGCGGTCAAAACACGAAGAG
OLG297—CGCTTCACTATCAACTGCTG
OLG298—TTTGCGGAGTTTCATCTACC

DNA sequencing was performed using a dye-terminator sequencing system (Perkin Elmer). Sequences of the many sequencing primers will be provided upon request. Products of sequencing reactions were analyzed by the Pharmacology Core facility at the University of Washington. Both strands of the cDNA were sequenced at least once. At least three independent clones of RT–PCR products were sequenced on both strands. These sequences were also confirmed by genomic sequences produced by the C. elegans genome project.

The *aex-3*::*gfp* fusion plasmid pTJ644 was constructed as follows. The HindIII–KpnI fragment (1.4 kb long) of pTJ500 was cloned into the HindIII and BamHI sites of pBluescript SK+ (the KpnI site of pTJ500 was converted to a BamHI site by treatment with T4 DNA polymerase and ligation of a BamHI linker). This HindIII–BamHI fragment was further subcloned into pPD95.69 (a GFP expression vector; a gift from A. Fire). Sequencing confirmed that codon 49 of *aex-3* was fused in frame to *gfp*.

Acknowledgments

We thank E. Hankins and P. Colacurcio for technical assistance; E. Jorgensen for the *n2166* allele and information about *ox3*; A. Fire for pPD95.69; L. Huang and P. Sternberg for pbHL98; A. Loewy and L. Salkoff for providing recording equipment; A. Coulson for cosmids; R. Barstead for the C. elegans cDNA library; D. Birnby for C. elegans RNA; the C. elegans Genome Sequencing Consortium for C. elegans genome sequences; C. Manoil for advice on protein structure; and M. Ailion, S. Bajjalieh, T. Inoue, D. Johnstone, E. Jorgensen, E. Malone, P. Swoboda, and K. Yook for comments on the manuscript. This work was supported by Public Health Service Grant R01NS30187 and R01NS32057 to J. H. T., NS09937 to J. S., and R01NS33535 to M. N. Some strains were obtained from the *Caenorhabditis* Genetics Center, which is funded by the National Institutes of Health National Center for Research Resources.

Received November 27, 1996; revised March 13, 1997.

References

Alfonso, A., Grundahl, K., Duerr, J.S., Han, H.P., and Rand, J.B. (1993). The *Caenorhabditis elegans unc-17* gene: a putative vesicular acetylcholine transporter. Science *261*, 617–619.

Alfonso, A., Grundahl, K., McManus, J.R., and Rand, J.B. (1994). Cloning and characterization of the choline acetyltransferase structural gene (*cha-1*) from C. elegans. J. Neurosci. *4*, 2290–2300.

Andres, D.A., Seabra, M.C., Brown, M.S., Armstrong, S.A., Smeland, T.E., Cremers, F.P., and Goldstein, J.L. (1993). cDNA cloning of component A of Rab geranylgeranyl transferase and demonstration of its role as a Rab escort protein. Cell *7*, 1091–1099.

Avery, L. (1993). The genetics of feeding in Caenorhabditis elegans. Genetics *133*, 897–917.

Avery, L., Raizen, D., and Lockery, S. (1995). Electrophysiological methods. In Methods in Cell Biology, Caenorhabditis elegans: Modern Biological Analysis of an Organism, H.F. Epstein and D.C. Shakes, eds. (San Diego, California: Academic Press, Inc.), pp. 251–269.

Bargmann, C.I., and Horvitz, H.R. (1991). Control of larval development by chemosensory neurons in Caenorhabditis elegans. Science *251*, 1243–1246.

Barstead, R.J., Kleiman, L., and Waterston, R.H. (1991). Cloning, sequencing, and mapping of an alpha-actinin gene from the nematode Caenorhabditis elegans. Cell Motil. Cytoskeleton *20*, 69–78.

Brenner, S. (1974). The genetics of Caenorhabditis elegans. Genetics *77*, 71–94.

Brondyk, W.H., McKiernan, C.J., Fortner, K.A., Stabila, P., Holz, R.W., and Macara, I.G. (1995). Interaction cloning of Rabin3, a novel protein that associates with the Ras-like GTPase Rab3A. Mol. Cell. Biol. *15*, 1137–1143.

Brose, N., Hofmann, K., Hata, Y., and Südhof, T.C. (1993). Mammalian homologues of *Caenorhabditis elegans unc-13* gene define novel family of C2-domain proteins. J. Biol. Chem. *270*, 25273–25280.

Burton, J.L., Burns, M.E., Gatti, E., Augustine, G.J., and DeCamilli, P. (1994). Specific interactions of Mss4 with members of the Rab GTPase subfamily. EMBO J. *13*, 5547–5558.

deHoop, M.J., Huber, L.A., Stenmark, H., Williamson, E., Zerial, M., Parton, R.G., and Dotti, C.G. (1994). The involvement of the small GTP-binding protein Rab5a in neuronal endocytosis. Neuron *13*, 11–22.

Ferro-Novick, S., and Novick, P. (1993). The role of GTP-binding proteins in transport along the exocytic pathway. Annu. Rev. Cell Biol. *9*, 575–599.

Fischer von Mollard, G., Südhof, T.C., and Jahn, R. (1991). A small GTP-binding protein dissociates from synaptic vesicles during exocytosis. Nature *349*, 79–91.

Fischer von Mollard, G., Stahl, B., Walch-Solimena, C., Takei, K., Daniels, L., Khoklatchev, A., DeCamilli, P., Südhof, T.C., Jahn, R. (1994a). Localization of Rab5 to synaptic vesicles identifies endosomal intermediate in synaptic vesicle recycling pathway. Eur. J. Cell Biol. *65*, 319–326.

Fischer von Mollard, G., Khoklatchev, A., Stahl, B., Südhof, T.C., and Jahn, R. (1994b). Rab3C is a synaptic vesicle protein that dissociates from synaptic vesicles after stimulation of exocytosis. J. Biol. Chem. *269*, 10971–10974.

Fleming, J.T., Tornoe, C., Riina, H.A., Coadwell, J., Lewis, J.A., and Sattelle, D.B. (1993). Acetylcholine receptor molecules of the nematode Caenorhabditis elegans. Comp. Mol. Neurobiol. *63*, 65–80.

Gengyo-Ando, K., Kamiya, Y., Yamakawa, A., Kodaira, K., Nishiwaki, K., Miwa, J., Hori, I., and Hosono, R. (1993). The C. elegans *unc-18* gene encodes a protein expressed in motor neurons. Neuron *11*, 703–711.

Geppert, M., Bolshakov, V.Y., Siegelbaum, S.A., Takei, K., DeCamilli, P., Hammer, R.E., and Südhof, T.C. (1994a). The role of Rab3A in neurotransmitter release. Nature *369*, 493–497.

Hall, D.H., and Hedgecock, E.M. (1991). Kinesin-related gene unc-104 is required for axonal transport of synaptic vesicles in C. elegans. Cell *65*, 837–847.

Hata, Y., Slaughter, C.A., and Südhof, T.C. (1993). Synaptic vesicle fusion complex contains *unc-18* homologue bound to syntaxin. Nature *366*, 347–351.

Hodgkin, J. (1983). Male phenotypes and mating efficiency in C. elegans. Genetics *103*, 43–64.

Horvitz, H.R., Brenner, S., Hodgkin, J., and Herman, R.K. (1979). A uniform genetic nomenclature for the nematode Caenorhabditis elegans. Mol. Gen. Genet. *175*, 129–133.

Huang, L.-S., Tzou, P., and Sternberg, P.W. (1994). The lin-15 locus encodes two negative regulators of Caenorhabditis elegans vulval development. Mol. Biol. Cell *5*, 395–411.

Johannes, L., Lledo, P.M., Roa, M., Vincent, J.D., Henry, J.P., and Darchen, F. (1994). The GTPase Rab3a negatively controls calcium-dependent exocytosis in neuroendocrine cells. EMBO J. *13*, 2029–2037.

Johnston, P.A., Archer, B.T., III, Robinson, K., Mignery, G.A., Jahn, R., and Südhof, T.C. (1991). rab3A attachment to the synaptic vesicle membrane mediated by a conserved polyisoprenylated carboxy-terminal sequence. Neuron *7*, 101–109.

Kyte, J., and Doolittle, R.F. (1982). A simple method for displaying the hydropathic character of a protein. J. Mol. Biol. *157*, 105–132.

Lewis, J.A., Wu, C.H., Berg, H., and Levine, J.H. (1980). The genetics of levamisole resistance in the nematode Caenorhabditis elegans. Genetics *95*, 905–928.

Lichy, J.H., Modi, W.S., Seuanez, H.N., and Howley, P.M. (1992). Identification of a human chromosome 11 gene which is differentially

regulated in tumorigenic and nontumorigenic somatic cell hybrids of HeLa cells. Cell Growth Differ. *3*, 541–548.

Liu, D.W., and Thomas, J.H. (1994). Regulation of a periodic motor program in C. elegans. J. Neurosci. *14*, 1953–1962.

Livingstone, D. (1991). Studies on the *unc-31* gene of Caenorhabditis elegans. Ph.D. dissertation. University of Cambridge.

Maruyama, I.N., and Brenner, S.A. (1991). A phorbol ester/diacylglycerol-binding protein encoded by the *unc-13* gene of *Caenorhabditis elegans*. Proc. Natl. Acad. Sci. USA *88*, 5729–5733.

McIntire, S.L., Jorgensen, E., and Horvitz, H.R. (1993). Genes required for GABA function in *Caenorhabditis elegans*. Nature *364*, 334–337.

Mello, C.C., Kramer, J.M., Stinchcomb, D., and Ambros, V. (1991). Efficient gene transfer in C. elegans: extrachromosomal maintenance and integration of transforming sequences. EMBO J. *10*, 3959–3970.

Miller, K.G., Alfonso, A., Nguyen, M., Crowell, J.A., Johnson, C.D., and Rand, J.B. (1996). A genetic selection for *Caenorhabditis elegans* synaptic transmission mutants. Proc. Natl. Acad. Sci. USA *93*, 12593–12598.

Nguyen, M., Alfonso, A., Johnson, C.D., and Rand, J.B. (1995). Caenorhabditis elegans mutants resistant to inhibitors of acetylcholinesterase. Genetics *140*, 527–535.

Nonet, M.L., Grundahl, K., Meyer, B.J., and Rand, J.B. (1993). Synaptic function is impaired but not eliminated in C. elegans mutants lacking synaptotagmin. Cell *73*, 1291–1305.

Oberhauser, A.F., Monck, J.R., Balch, W.E., and Fernandez, J.M. (1992). Exocytotic fusion is activated by Rab3a peptides. Nature *360*, 270–273.

Okada, Y., Yamazaki, H., Sekine-Aizawa, Y., and Hirokawa, N. (1995). The neuron-specific kinesin superfamily protein KIF1A is a unique monomeric motor for anterograde axonal transport of synaptic vesicle precursors. Cell *81*, 769–780.

Olszewski, S., Deeney, J.T., Schuppin, G.T., Williams, K.P., Corkey, B.E., and Rhodes, C.J. (1994). Rab3A effector domain peptides induce insulin exocytosis via a specific interaction with a cytosolic protein doublet. J. Biol. Chem. *269*, 27987–27991.

Raizen, D.M., and Avery, L. (1994). Electrical activity and behavior in the pharynx of Caenorhabditis elegans. Neuron *12*, 483–495.

Raizen, D.M., Lee, R.Y.N., and Avery, L. (1995). Interacting genes required for pharyngeal excitation by motor neuron MC in Caenorhabditis elegans. Genetics *141*, 1365–1382.

Salminen, A., Novick, P.J. (1987). A ras-like protein is required for a post-Golgi event in secretion. Cell *49*, 527–538.

Sambrook, J., Fritsch, E.F., and Maniatis, T. (1989). Molecular Cloning, A Laboratory Manual. (Cold Spring Harbor, New York: Cold Spring Harbor Laboratory Press).

Sasaki, T., Kikuchi, A., Araki, S., Hata, Y., Isomura, M., Kuroda, S., and Takai, Y. (1990). Purification and characterization from bovine brain cytosol of a protein that inhibits the dissociation of GDP from and the subsequent binding of GTP to smg p25A, a ras p21-like GTP-binding protein. J. Biol. Chem. *265*, 2333–2337.

Schackwitz, W., Inoue, T., and Thomas, J.H. (1996). Sensory neurons function in parallel to regulate development in C. elegans. Neuron *17*, 719–728.

Seabra, M.C., Brown, M.S., Slaughter, C.A., Sudhof, T.C., and Goldstein, J.L. (1992). Purification of component A of Rab geranylgeranyl transferase: possible identity with the choroideremia gene product. Cell *70*, 1049–1057.

Segev, N., Mulholland, J., Botstein, D. (1988). The yeast GTP-binding YPT1 protein and a mammalian counterpart are associated with the secretion machinery. Cell *52*, 915–924.

Shirataki, H., Kaibuchi, K., Sakoda, T., Kishida, S., Yamaguchi, T., Wada, K., Miyazaki, M., and Takai, Y. (1993). Rabphilin-3A, a putative target protein for smg p25A/rab3A p25 small GTP-binding protein related to synaptotagmin. Mol. Cell. Biol. *13*, 2061–2068.

Stahl, B., von Mollard, G.F., Walch-Solimena, C., and Jahn, R. (1994). GTP cleavage by the small GTP-binding protein Rab3A is associated with exocytosis of synaptic vesicles induced by alpha-latrotoxin. J. Biol. Chem. *269*, 24770–24776.

Südhof, T.C. (1995). The synaptic vesicle cycle: a cascade of protein–protein interactions. Nature *375*, 645–653.

Sulston, J., and Hodgkin, J. (1988). Methods Appendix in The Nematode Caenorhabditis elegans. W. Wood, ed. (Cold Spring Harbor, New York: Cold Spring Harbor Laboratory).

Thomas, J.H. (1990). Genetic analysis of defecation in Caenorhabditis elegans. Genetics *124*, 855–872.

Thomas, J.H. (1993). Chemosensory regulation of development in C. elegans. Bioessays *15*, 791–797.

Vowels, J.J., and Thomas, J.H. (1992). Genetic analysis of chemosensory control of dauer formation in Caenorhabditis elegans. Genetics *130*, 105–123.

Walent, J.H., Porter, B.W., and Martin, T.F. (1992). A novel 145 kd brain cytosolic protein reconstitutes Ca(2+)-regulated secretion in permeable neuroendocrine cells. Cell *70*, 765–775.

White, J.G., Southgate, E., Thomson, J.N., and Brenner, S. (1976). The structure of the ventral nerve cord of Caenorhabditis. Philos. Trans. R. Soc. Lond. [Biol.] *275B*, 327–348.

Wilson, R., Ainscough, R., Anderson, K., Baynes, C., Berks, M., Burton, J., Connell, M., Bonfield, J., Copsey, T., and Cooper, J. (1994). 2.2 Mb of contiguous nucleotide sequence from chromosome III of C. elegans. Nature *368*, 32–38.

Yu, H., Chen, J.K., Feng, S., Dalgarno, D.C., Brauer, A.W., and Schreiber, S.L. (1994). Structural basis for the binding of proline-rich peptides to SH3 domains. Cell *76*, 933–945.

GenBank Accession Number

The GenBank accession number for *aex-3* sequence is U93842.

Note Added in Proof

A paper describing the purification of a protein that is nearly identical to DENN and 35% identical to *aex-3* has recently been published (Wada, M., Nakanishi, H., Satoh, A., Hirano, H., Obaishi, H., Matsuura, Y., and Takai, Y. (1997). Isolation and characterization of a GDP/GTP exchange protein specific for the Rab3 subfamily small G proteins. J. Biol. Chem. *272*, 3875–3878). This protein is shown to have guanine-nucleotide exchange activity specifically for Rab3A, Rab3C, and Rab3D, indicating that AEX-3 is likely to have a similar function for RAB-3.